JOURNAL OF DYNAMICS AND CONTROL

VOLUME 8 ISSUE 8

PROLIFIC, CHARACTERIZED AND HYPOTHETICAL EVALUATION OF GUANINE DERIVATIVE 2-AMINO-9-(4-ISOPROPYLBENZYL)-1, 9-DIHYDROPURIN-6-ONE

Shanmugasundari. M[1*], Vijaya. P[2], Bhaskar. T[3], Banumathi. N[4]

[1]Research scholar, [2,3,4]Assistant Professor, Department of Chemistry, Rani Anna Government College for Women, Tirunelveli-8, Affiliated to Manonmaniam Sundaranar University, Tirunelveli - 627 012, India

PROLIFIC, CHARACTERIZED AND HYPOTHETICAL EVALUATION OF GUANINE DERIVATIVE 2-AMINO-9-(4-ISOPROPYLBENZYL)-1, 9-DIHYDROPURIN-6-ONE

Shanmugasundari. M[1*], Vijaya. P[2], Bhaskar. T[3], Banumathi. N[4]

[1]Research scholar ([Reg. No. 20211172032001], ORCID: 0009-0001-0531-5859), [2,3,4]Assistant Professor

Department of Chemistry, Rani Anna Government College for Women, Tirunelveli-8,
Affiliated to Manonmaniam Sundaranar University, Tirunelveli - 627 012, India
[1]shanmugasundarichemistry@gmail.com, [2]racchemonlineclass@gmail.com, [3]bhas51@yahoo.com, [4]mobapra33@yahoo.co.in

ABSTRACT: Guanine is one of the derivatives that are critical building blocks for DNA and RNA. The pharmacological properties of cuminaldehyde are used in the development of new medications. The guanine derivative 2-amino-9-(4-isopropylbenzyl)-1,9-dihydropurin-6-one (GD) is synthesised and DFT calculations are performed using the Gaussion 03 software package. B3LYP functional with the basis set 6-31G (d, p) is used for the theoretical investigation of the molecule GD. The calculated IR frequencies, UV absorbance and NMR chemical shifts are found to be in accordance with experimental values. The molecular properties, such as dipole moment, and polarizabilities, are calculated at the same level of computation.

KEYWORDS: Guanine derivative, frequency, NMR, DFT

1. INTRODUCTION

Guanine derivatives have a lot of biological action because they are effective at inhibiting viral DNA [1-2]. The pharmacophore model, AARR, proposed based on the common feature alignment, demonstrates that the drug ability of the guanine derivatives is provided by two fused rings, like in guanine, and two acceptors—one from keto-oxygen and the other from the substituent connected to nitrogen in imidazole ring [3]. Cuminaldehyde is an organic compound found in the essential oil of cumin, eucalyptus, myrrh and cassia. It possesses several biological properties, including antimicrobial, antioxidant, anti-inflammatory, and anticancer activities [4-5]. There are numerous guanine derivatives that have been synthesised and studied for their medicinal properties. These derivatives often exhibit enhanced pharmacological effects compared to guanine itself. They have been explored in the treatment of various diseases, including cancer, viral infections, and neurodegenerative disorders [6-13]. In this present study, the compound GD is newly synthesized using guanine and cuminaldehyde. GD is spectrally characterised by IR, UV, and NMR spectroscopy.

2. MATERIALS AND METHODS

2.1 Synthesis

0.001 mol of guanine in KOH solution and 0.001 mol of cuminaldehyde in ethanol are mixed together in a 250 ml RB flask. This solution is refluxed for 50 minutes at 60^{o}C until the colour changes to a dark red orange solution. Then the compound is allowed to dry and recrystallized using ethanol. The obtained compound (Yield – 73%) is used for spectral evaluation. The systematic reaction is represented below.

In this reaction, cuminaldehyde reacts with KOH and forms the 4-isopropyl benzoic acid by converting the –CHO group into –COOH. Then the –COOH group reacts with guanine's –NH to form the product by eliminating H_2O.

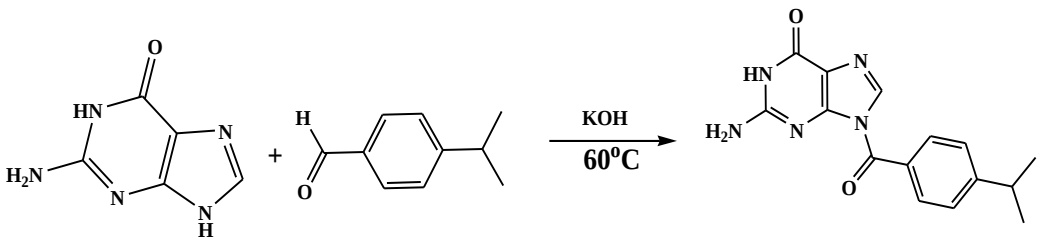

Guanine Cuminaldehyde 2-amino-9-(4-isopropylbenzyl)-1,9-dihydropurin-6-one

Scheme 1. Systematic preparation of 2-amino-9-(4-isopropylbenzyl)-1,9-dihydropurin-6-one

2.2 Spectral measurement

The obtained guanine derivative is subjected to IR, UV-vis, and NMR spectral evaluation. The IR spectrum of the guanine derivative is recorded by an FT-IR spectrometer as KBr pelletization method. The absorbance is recorded by UV-Vis spectrometer using ethanol as a solvent. The NMR is recorded at 500 MHz on a Bruker NMR with DMSO solvent.

2.3 Computational techniques

The Gaussian 03W software suite is used to conduct all DFT research [14-16]. Applying the B3LYP/DFT 6-31G (d,p) basis set, the synthesised structure is designed and optimised to geometry with minimal energy.

The optimised structure is put through a frequency computation using the same basis set mentioned above. The scaling factor of 0.9614 is used to transform the unscaled frequency into the scaled frequency. Veda4 software is used to determine the molecule's potential energy difference (PED)% [17].

NMR calculations are performed on the optimised structure using the 6-311+G (2d,p) basis set and DMSO as the solvent. The respective scaling factors for the ^{13}C and ^{1}H NMR chemical shifts are 181.6032 and 31.7838.

Natural bond orbital and polarizability calculations are performed using the 6-31G (d,p) basis set. HOMO, LUMO, and MEP surfaces of GD are also visualised [18-19]. The anti-bacterial studies were carried out by PASS online software.

3. RESULT AND DISCUSSION

3.1 Geometry optimization

A 6-31G(d,p) basis set DFT/B3LYP computation is used to develop and optimise the synthesised molecule structure for least ground energy. The molecule has 156 electrons and 37 atoms. **Figure 1** shows the optimal structure with numbering used for this study and **Table 1** lists the geometrical properties of 2-amino-9-(4-isopropylbenzyl)-1,9-dihydropurin-6-one, including bond angle, bond length, and torsion angle.

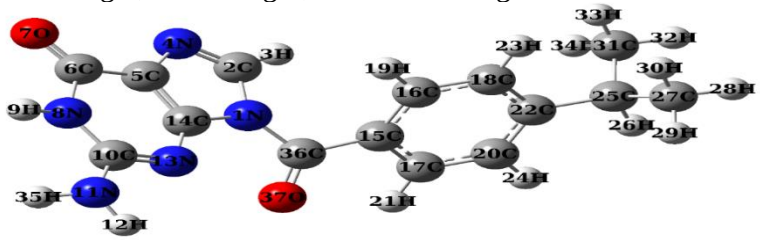

Figure 1. Numbering adopted for 2-amino-9-(4-isopropylbenzyl)-1,9-dihydropurin-6-one (GD)

Table 1. Selected geometric parameters of 2-amino-9-(4-isopropylbenzyl)-1,9-dihydropurin-6-one computed by DFT method (B3LYP/6-31G(d,p))

Bond	**Bond length (Å)**	**Bonds**	**Bond angle (º)**
N1-C2	1.41	N1-C36-C15	116.5
N1-C14	1.39	N1-C36-O37	120.3
N1-C36	1.43	C2-N1-C36	127.0
C2-N4	1.30	C36-C15-C16	123.6
N4-C5	1.38	C22-C25-C27	111.6
C5-C6	1.44	C22-C25-C31	111.8
C5-C14	1.39	C27-C25-C31	111.1
C6-O7	1.22	-	-
C6-N8	1.43	-	-
N8-C10	1.37	-	-
C10-N11	1.37	-	-
C10-N13	1.31	**Bonds**	**Torsion angle (º)**
N13-C14	1.35	N1-C36-C15-C17	28.84
C15-C36	1.49	C2-N1-C36-O37	-142.1
C22-C25	1.52	C16-C15-C36-O37	-151.4
C25-C27	1.54	C20-C22-C25-C27	-115.7
C25-C31	1.54	C20-C22-C25-C31	119.1
C36-O37	1.21	-	-

3.2 FT-IR calculations

An IR frequency calculation is performed on the optimised structure, which reveals 105 vibrational modes, 36 stretching modes, 35 bending modes, 34 torsion modes, and 36 CH modes. The modes are shown in the positive region, indicating that the molecule is in a ground state of minimal energy and stable conformation. The molecule has C1 symmetry. **Figure 2** displays the experimental vibrational spectra.

The band around 3418 cm^{-1} indicates the N-H stretching, and 3065, 2961, 2925 cm^{-1} implies the C-H stretching of the compound GD. A broad band appears at 1627, 1603 cm^{-1} displayed the C=O stretching, and 1561 cm^{-1} implies the C-N stretching in the compound. The C-C stretching arises at 1495, 1437, 1410 cm^{-1}. These experiments are well aligned with theoretical IR frequencies (**Table 2**).

Table 2. Significant Vibrational wavenumbers obtained for 2-amino-9-(4-isopropylbenzyl)-1,9-dihydropurin-6-one at B3LYP/6-31G(d,p) level of calculations

Mode No.	Theoretical Frequency (cm^{-1}) DFT /B3LYP /6-31G(d,p)		Experimental Frequency (cm^{-1})	Vibrational assignments PED ≥ 10
	Unscaled Frequency	Scaled Frequency		
1	3699	3556.2	3418.42	ν_{N11H12} (51%) + ν_{N11H35} (49%)
2	3601	3462.0		ν_{N8H9} (98%)
3	3581	3442.8		ν_{N11H12} (48%) + ν_{N11H35} (50%)
9	3125	3004.4	3064.66	ν_{C27H29} (34%) + ν_{C31H34} (36%) + ν_{N13C10} (18%)
11	3117	2996.7		ν_{C27H28} (22%) + ν_{C27H30} (23%) + ν_{C31H32} (26%) + ν_{C31H33} (27%)

13	3046	2928.4	2961.35 2925.96	ν_{C27H28} (15%) + ν_{C27H29} (13%) + ν_{C27H30} (15%) + ν_{C32H32} (20%) + ν_{C31H33} (20%) + ν_{C31H34} (17%)
14	3042	2924.6		ν_{C27H28} (20%) + ν_{C27H29} (15%) + ν_{C27H30} (21%) + ν_{C31H32} (15%) + ν_{C31H33} (16%) + ν_{C31H34} (12%)
16	1829	1758.4	1626.64	ν_{O7C6} (74%) + $\beta_{C6N8C10}$ (12%)
17	1800	1730.5	1603.12	ν_{O37C36} (88%)
18	1673	1608.4	1561.60	ν_{N1C10} (24%) + ν_{N11C10} (17%) + $\beta_{H35N11H12}$ (40%)
19	1662	1597.8	1495.92	ν_{C16C18} (29%) + ν_{C17C20} (12%) + ν_{C22C20} (11%)
20	1619	1556.5	1456.40	ν_{N13C10} (29%) + $\beta_{H35N11H12}$ (35%)
21	1616	1553.6	1437.39	ν_{C15C17} (21%) + ν_{C22C20} (24%) + $\beta_{C16C18C22}$ (10%)
22	1592	1530.5	1410.36	ν_{C5C4} (36%) + ν_{N13C14} (24%)
23	1560	1499.8	1384.96	ν_{N4C2} (54%) + β_{H3C2N4} (10%)
31	1442	1386.3	1355.68	ν_{C5C14} (13%) + ν_{N8C10} (14%) + ν_{N1C14} (13%) + $\beta_{N13C14C5}$ (11%) + $\beta_{N4C5C14}$ (16%)
35	1368	1315.2	1319.29	ν_{N1C14} (16%) + ν_{N1C36} (11%) + β_{H3C2N4} (16%)
38	1344	1292.1	1307.02	ν_{C15C17} (13%) + ν_{N4C5} (18%)
39	1324	1272.9	1293.20	ν_{N11C10} (17%) + $\beta_{H9N8C10}$ (41%) + β_{H3C2N4} (13%)
41	1304	1253.7	1226.09	ν_{N1C36} (10%) + ν_{C36C15} (21%) + β_{H3C2N4} (18%)
43	1224	1176.8	1162.84	β_{C2N4C5} (12%) + $\beta_{H23C18C16}$ (11%) + $\beta_{H24C20C17}$ (10%) + $\beta_{C5C14N1}$ (12%)
44	1217	1170.0	1154.27	β_{H3C2N4} (21%)
45	1200	1153.7	1128.02	ν_{N1C14} (10%) + ν_{C36C15} (11%) + $\beta_{H19C16C18}$ (19%)
47	1147	1102.7	1073.98	ν_{N13C10} (11%) + ν_{N4C5} (13%) + ν_{N8C6} (17%) + $\beta_{H12N11C10}$ (18%)
51	1080	1038.3	1025.11	$\nu_{C18C224}$ (16%) + $\tau_{H30C27C25C31}$ (14%) + $\tau_{H33C31C25C27}$ (13%)
52	1060	1019.1	1003.81	ν_{N8C10} (11%) + ν_{N8C6} (27%) + $\beta_{N4C5C14}$ (10%)
59	921	885.4	913.13	β_{C2N4C5} (25%) + $\beta_{O37C36C15}$ (15%)
63	842	809.5	848.86	ν_{N13C14} (10%) + ν_{N4C5} (18%) + $\beta_{N8C10N13}$ (14%)
65	784	753.7	778.94	$\tau_{C15C17C20C22}$ (12%) + $\gamma_{O37N1C15C36}$ (32%)
66	773	743.2	746.10	$\gamma_{O7N8C5C6}$ (25%) + $\gamma_{N13N1C5C14}$ (12%)
69	722	694.1	699.24	$\tau_{C16C18C22C20}$ (11%) + $\tau_{C15C17C20C22}$ (21%) + $\tau_{C18C22C20C17}$ (11%) + $\gamma_{O37N1C15C36}$ (20%)
70	705	677.8	682.67	$\tau_{H9N8C10N11}$ (12%) + $\gamma_{O7N8C5C6}$ (13%) + $\gamma_{N11N8N13C10}$ (10%)
71	675	648.9	604.71	$\tau_{C2N4C5C14}$ (23%)
76	606	582.6	572.53	$\tau_{H9N8C10N11}$ (62%)

77	578	555.7	525.26	$\tau_{H12N11C10N8}$ (55%)
78	562	540.3	469.57	$\beta_{C6N8C10}$ (10%) + $\tau_{H12N11C10N8}$ (19%)
88	337	324.0		$\tau_{H12N11C10N8}$ (12%) + $\tau_{H35N11C10N8}$ (66%)

ν –stretching vibration; β – bending vibration; τ – torsion; γ – out – of – plane bending.

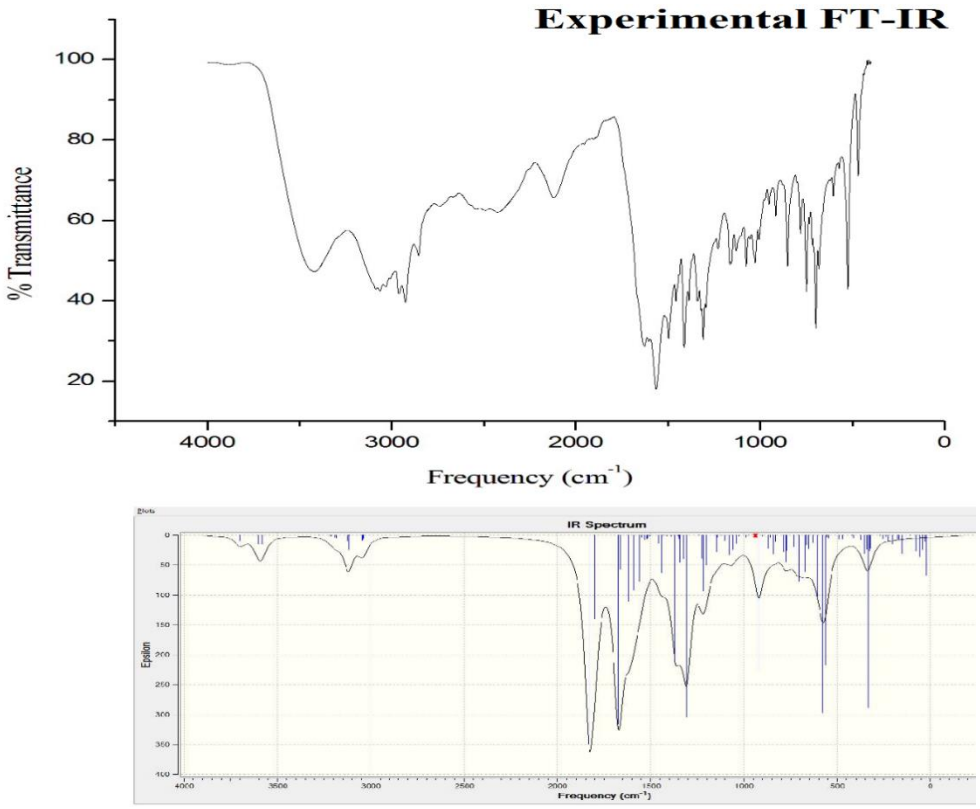

Figure 2. Experimental and theoretical vibrational spectra of 2-amino-9-(4-isopropylbenzyl)-1,9-dihydropurin-6-one

3.3 UV-vis analysis

The synthesized GD compound is analyzed using a UV-visible spectrophotometer with ethanol as the solvent. The synthesized compound exhibits a high absorbance at 325 nm and 283 nm. These values are in agreement with the theoretical values of 369 nm, 294 nm, and 269 nm, respectively, which were calculated using TD-SCF [scrf=(solvent=Ethanol)]. The experimental and theoretical absorbance and their respective energy contributions for GD were illustrated in **Figure 3** and tabulated in **Table 3**. The major contribution (97%) of GD energy involved in the HOMO to LUMO transition is at 369 nm, while the minor contribution (2%) of energy involved is from the H-1 to L+1 energy levels at 269 nm.

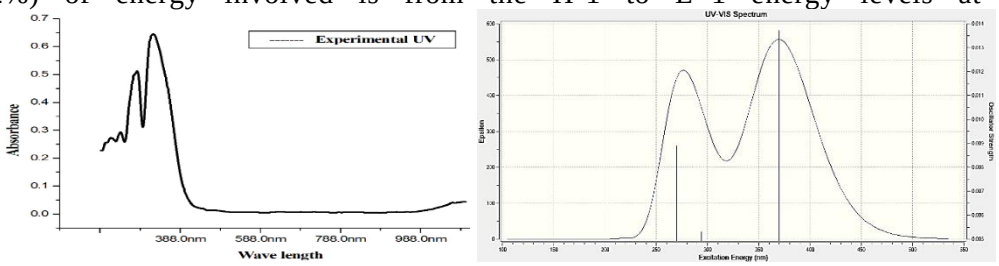

Figure 3. UV-vis spectrum of GD

Table 3. Absorbance and contributions of GD computed by B3LYP/6-31G (d,p) TD-SCF DFT method

Name	Energy (cm^{-1})	Experimental value λ_{max} (nm)	Major contributes	Minor contribute
GD	27039.9	325	HOMO→LUMO (97%)	-
	34009.4	283	H-5→LUMO (55%) H-2→LUMO (23%)	H-3→LUMO (7%) H-1→LUMO (3%)
	37068.7		H-1→LUMO (79%) H-4→LUMO (8%)	H-3→LUMO (6%) H-1→L+2 (2%)

3.4 NMR calculations

The key to understanding or predicting the compound's entire structural bonding is through NMR spectrum studies. The 6-311++G (d,2p) basis set is used for the ^{1}H NMR and ^{13}C NMR calculations of the GIAO shift in DMSO [scrf=(solvent=DMSO)]. **Table 4** compares the chemical shift of the molecule between experimental and theoretical data.

The ^{1}H NMR (**Figure 5**) and ^{13}C NMR (**Figure 4**) of GD have been recorded in DMSO shown in. The low field signal observed at 24.09 and 26.14 ppm indicates the isopropyl carbon of C31 and C27. The peak observed at 33.88 ppm indicates C25 carbon. The aromatic C peak of cuminaldehyde arises in the range of 127.44 to 139.03 ppm, and the C22, which is attached to isopropyl group, appeared at 158.52 ppm. The C36 of C=O appeared at 170.12 ppm. The aromatic carbon in the guaninyl part of the derivative appears in the range of 125.36 to 154.77 ppm. The methyl proton of GD is recorded in the range of 1.18, 1.20, and 1.23 ppm. Here the two methyl protons merge and gives a triplet peak. The single proton of H26 was observed at 2.88 ppm. The amine group of guanine protons is shown at 3.46 ppm. The aromatic protons are in the range of 7.07-7.79 ppm. They also agree quite well with one another.

Table 4. ^{1}H and ^{13}C NMR Chemical Shift for 2-amino-9-(4-isopropylbenzolyl)-1,9 dihydropurin-6-one computed by B3LYP/6-311+G(2d,p) GIAO DFT method

C	Theoretical chemical shift (ppm)	Experimental chemical Shift (ppm)	**H**	Theoretical chemical shift (ppm)	Experimental chemical shift (ppm)
C36	174.04	170.12	H9	8.50	7.79-7.07
C22	166.54	158.52	H21	8.50	
C6	161.94	154.77	H19	8.00	
C10,C14	159.64	149.03	H3	7.90	
C2	144.24	143.08	H24	7.80	
C17,C16,C15	137.94	139.03	H23	7.80	
C15	135.24	129.54	H12,H35	4.60	3.46
C20	134.04	129.15	H26	3.20	2.88
C18	130.04	127.44	H28,H33	1.30	1.23
C5	125.34	125.36	H32,H34	1.20	1.20
C25	40.34	33.88	H29,H30	1.10	1.18
C27	24.14	26.14	--	--	--
C31	23.84	24.09	--	--	--

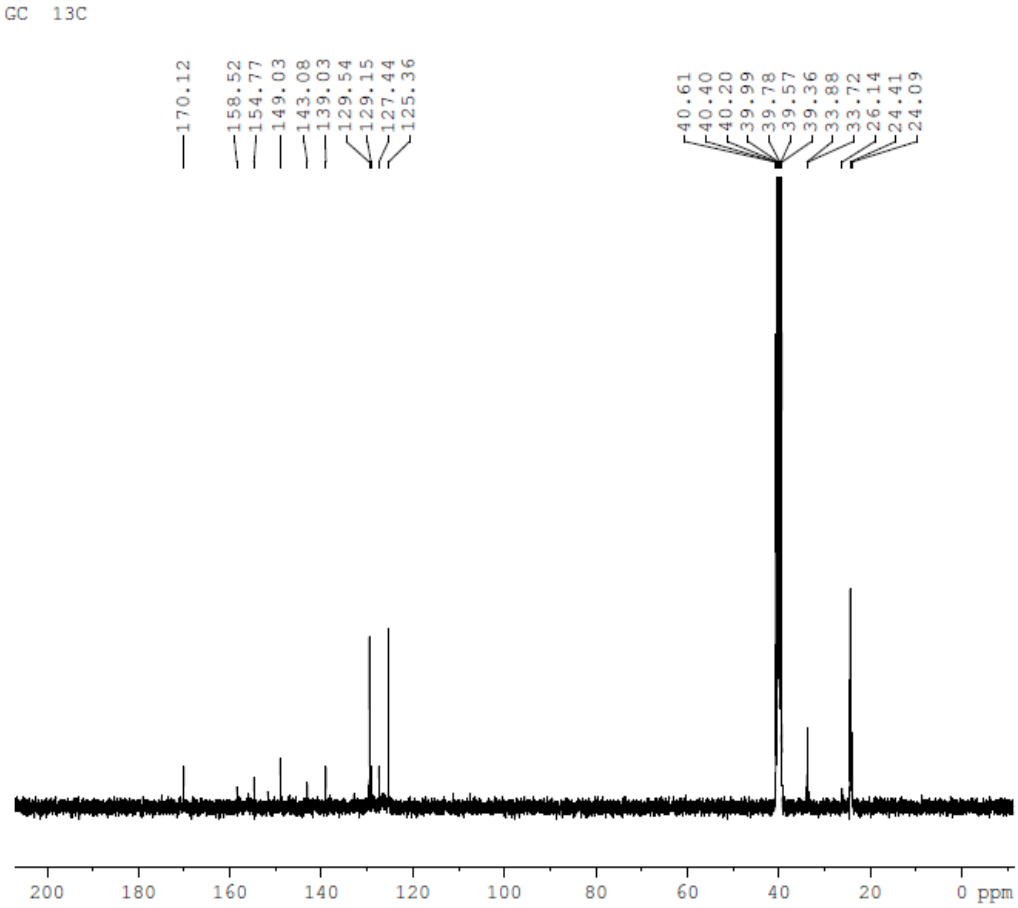

Figure 4. ^{13}C NMR spectrum of GD

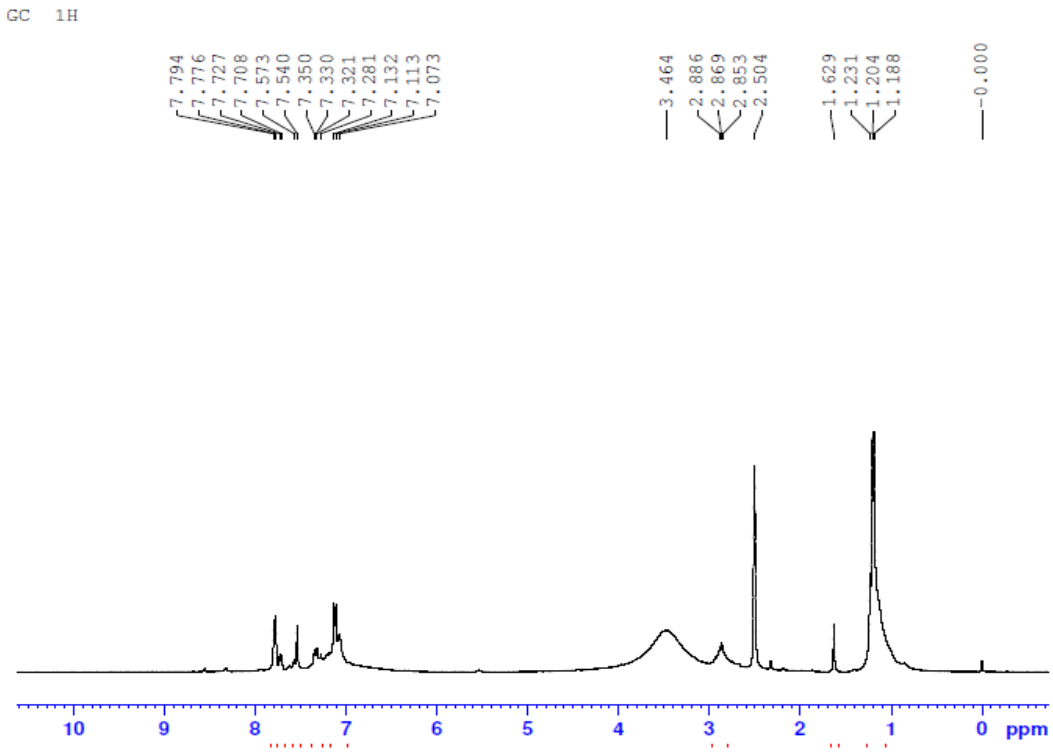

Figure 5. ^{1}H NMR spectrum of GD

3.5 NBO analysis

The second-order perturbation theory at the B3LYP/6-31G (d,p) basis set analyses the stabilisation energy of donor-acceptor interactions between the orbitals. **Table 5** comprises the E(2) value together with the donor bonding orbital (BD), acceptor antibonding orbital (BD*), and lone pair (LP) values. Energy stabilisation is directly correlated with the E(2) value. The compound's stronger delocalization electron occurs from the N8 atoms to the C10-N13 atoms with 61.6 kcal/mol energy. From N1-C2 to N13-C14, C2-N4 to C5-C6, C5-C14 to C10-N13, C10-N13 to N1-C4, N4 to C5-C14, and N13 to C5-C14, the lower delocalization of electrons varies from 5.45 to 10.16 kcal/mol. The lone pair electron of guanine N1 to C2-N4, C5-C14, C5-C14, and C36-O37 varies between 26.3-36.1 kcal/mol and, N4 to N1-C2, C5-C14 are 6.8 to 11.03 kcal/mol and, O7 to C5-C6, C6-N8 are 18.7-32.6 kcal/mol, N8 to C6-O7, C10-N13 have the highest delocalization of 42.7-61.6 kcal/mol, N11 to C10-N13 are 38.2 kcal/mol, and N13 to C5-C14, N8-C10 are 10.1-15.1 kcal/mol.

Table 5. Second order perturbation theory analysis of the fock matrix in NBO basis for 2-amino-9-(4-isopropylbenzyl)-1,9-dihydropurin-6-one

Donor NBO	Occupancy	Acceptor NBO (BD*)	Occupancy	E(2) in kcal/mol
(BD) C2-N4	1.98	C5-C14	0.22	15.99
(BD) C5-C14	1.84	C2-N4	0.14	17.02
(BD) C5-C14	1.84	C6-O7	0.17	29.55
(BD) C10-N13	1.89	C5-C14	0.22	26.00
(BD) C15-C17	1.80	C16-C18	0.16	21.45
(BD) C15-C17	1.80	C20-C22	0.17	17.30
(BD) C15-C17	1.80	C36-O37	0.10	18.89
(BD) C16-C18	1.82	C15-C17	0.19	17.94
(BD) C16-C18	1.82	C20-C22	0.17	21.43
(LP) N1	1.99	C2-N4	0.14	35.17
(LP) N1	1.99	C5-C14	0.22	36.11
(LP) N1	1.99	C36-O37	0.10	26.32
(LP) N4	1.99	N1-C2	0.05	11.03
(LP) O7	1.99	C5-C6	0.06	18.79
(LP) O7	1.99	C6-N8	0.10	32.66
(LP) N8	1.99	C6-O7	0.17	42.78
(LP) N8	**1.99**	**C10-N13**	**0.21**	**61.62**
(LP) N11	1.99	C10-N13	0.21	38.25
(LP) N13	1.99	C5-C14	0.22	10.16
(LP) N13	1.99	N8-C10	0.05	15.19
(LP) O37	1.99	N1-C36	0.10	32.06
(LP) O37	1.99	C15-C36	0.06	18.70

3.6 First-order molecular hyperpolarizability

The first hyperpolarizability of the molecule is calculated by B3LYP/6-31G (d,p) basis set on the finite field approach. The total dipole moment (μ), mean polarizability (α), and first hyperpolarizability (β) are calculated as follows,

$$\mu = (\mu_x^2 + \mu_y^2 + \mu_z^2)^{1/2} \quad (1)$$

$$\langle\alpha\rangle = \frac{1}{2}(\alpha_{xx} + \alpha_{yy} + \alpha_{zz}) \quad (2)$$

$$\beta_{tot} = [(\beta_{xxx} + \beta_{xyy} + \beta_{xzz})^2 + (\beta_{yyy} + \beta_{yzz} + \beta_{xxy})^2 + (\beta_{zzz} + \beta_{xxz} + \beta_{yyz})^2]^{1/2} \quad (3)$$

The calculated electric dipole moment μ (D), the mean polarizability <α> (x 10^{-24} esu) and the first hyperpolarizability β_{tot} (x10^{-33} esu) of 2-amino-9-(4-isopropylbenzyl)-1,9-dihydropurin-6-one are

tabulated in **Table 6.** The total molecular dipole moment (μ) and mean first hyperpolariability (β_{tot}) are 1.905 and 0.5486 x 10^{-30} esu, respectively, which are 1.5 times greater than the urea (0.3728 x 10^{-30}) value which shows that the molecule GD is considered to have NLO properties.

Table 6. The electric dipole moment μ (D), the mean polarizability <α> (x 10^{-24} esu) and the First hyperpolarizability β_{tot} (x10^{-33} esu) of GD by DFT method

Parameter	Value	Parameter	Value
μ_x	1.017	β_{xxx}	-659.01
μ_y	-1.519	β_{xxy}	-162.16
μ_z	0.536	β_{xyy}	164.55
μ	**1.905**	β_{yyy}	-62.965
α_{xx}	308.80	β_{xxz}	-167.42
α_{xy}	6.903	β_{xyz}	-36.488
α_{yy}	182.94	β_{yyz}	-34.945
α_{xz}	-12.909	β_{xzz}	31.909
α_{yz}	7.722	β_{yzz}	34.193
α_{zz}	117.07	β_{zzz}	-22.550
<α>	**202.94**	**β_{tot}**	**548.64**

α: 1a.u = 0.1482*10^{-24} esu , β: 1a.u = 8.6393*10^{-33} esu

3.7 MEP surface analysis

The MEP surface is generated by calculating the electron density and electrostatic potential of a molecule using DFT methods. The resulting MEP surface can provide insight into the reactivity and chemical properties of a molecule. This information is particularly useful in drug discovery and design, as it helps researchers predict how a molecule will interact with other biological molecules within a system. The positive region is displayed in blue and is open to nucleophilic attack, whereas the negative region is shown in red and is open to electrophilic attack. N11 and N8 are subject to nucleophilic attack, while O7 and O37 are electrophilic attack sites. The green area represents a potential middle ground between the two extremes of red and blue. The range of the MEP diagram for the substance under study is from -7.517e-2 (red) to +7.517e-2 (blue) units. The MEP surfaces of the compound shown in **Figure 6**.

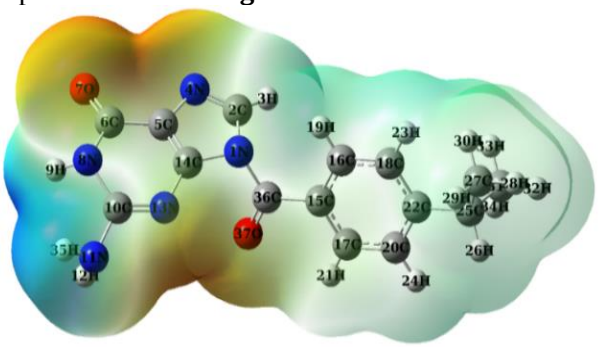

Figure 6. Neutral MEP surface of 2-amino-9-(4-isopropylbenzyl)-1,9-dihydropurin-6-one

3.8 FMO analysis

The frontier orbital gap simplifies characterizing the chemical reactivity and kinetic stability of the molecule. The electron acceptor is the lowest unoccupied molecular orbital (LUMO) **Figure 7** and the electron donor is the highest occupied molecular orbital (HOMO) which is shown in **Figure 8**.

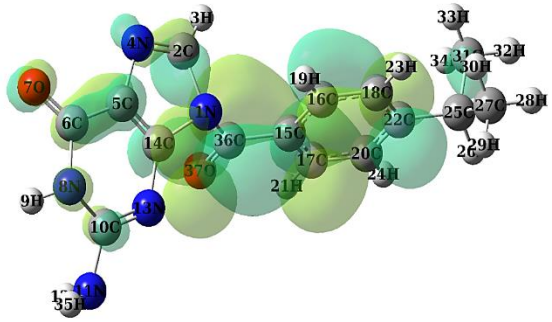

Figure 7. LUMO picture of 2-amino-9-(4-isopropylbenzyl)-1,9-dihydropurin-6-one

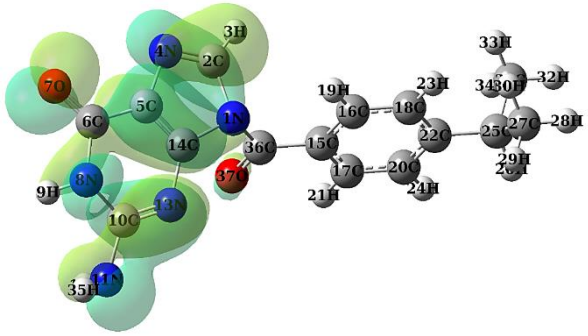

Figure 8. HOMO picture of 2-amino-9-(4-isopropylbenzyl)-1,9-dihydropurin-6-one

All atoms except N11, C25, and C27 involved are in LUMO formation. Only the guanine molecule with O37 atoms is involved in HOMO formation. The HOMO and LUMO energy levels of 2-amino-9-(4-isopropylbenzyl)-1,9-dihydropurin-6-one are -5.741 eV and -1.774 eV, respectively. The energy gap between HOMO and LUMO is 3.968 eV, which is responsible for chemical hardness or softness and tells about the reactivity, stability of the molecule.

The HOMO energy and average HOMO and LUMO energies are connected to electronegativity and ionisation potential, respectively. Hardness and the band gap energy are related. Consequently, the following formulas can be used to compute the electronegativity (χ), chemical hardness (η), softness (S) chemical potential (σ), and globalphilicity (ω):

$$\eta = \tfrac{1}{2}[E_L - E_H] \quad (4)$$

$$S = \tfrac{1}{2}\eta \quad (5)$$

$$\sigma = -E_H \quad (6)$$

$$\chi = -E_L \quad (7)$$

$$\omega = \sigma^2/2\,\eta \quad (8)$$

The calculated values are represented in **Table 7.**

Table 7. Calculated Chemical hardness (η), Chemical softness (S), Chemical potential (σ), Electro negativity (χ) and globalphilicity (ω) of the molecule GD

HOMO (eV)	LUMO (eV)	Bandgap energy (eV)	η	S	σ	χ	ω
-5.7412	-1.7736	3.9676	1.9838	0.9919	5.7412	1.7736	8.3076

3.9 Anti-bacterial studies

The anti-bacterial insilico trials are conducted over one or more of the 353 microorganisms at concentrations lower than 10,000 nM. **Table 8** provides the result as an activity percentage of GD, revealing good activity of 60% against Streptococcus viridians, which occurs frequently in the gastrointestinal system, upper respiratory tract, and oral cavity. When it comes to Escherichia coli K12 and Corynebacterium jeikeium, the GD has above 30% activity against both gram-positive and gram-negative bacteria. The other bacterial activity, such as those of Propionibacterium acnes

(19.9%), Mycobacterium avium (15%), Enterococcus sp. (8%), Sarcina (4.9%), Yersinia pseudotuberculosis (3%) and Fusobacterium nucleatum (1%), are less than 20% with GD.

Table 8. Anti-bacterial studies of GD with activity percentage

Bacteria	**Activity %**
Streptococcus viridians	60.13
Escherichia coli K12	36.19
Corynebacterium jeikeium	33.64
RESISTANT Propionibacterium acnes	19.95
Mycobacterium avium	15.44
Enterococcus sp.	8.57
Sarcina	4.91
Yersinia pseudotuberculosis	3.34
Fusobacterium nucleatum	1.54

4. CONCLUSION

The compound 2-amino-9-(4-isopropylbenzyl)-1,9-dihydropurin-6-one (GD) is synthesized and then studied by FT-IR , UV and NMR spectral analysis. The DFT B3LYP/6-31G (d, p) technique is used for the computational assignment. When compared to experimental data, the frequency calculations, UV, and NMR calculations are in good agreement. The molecule's first hyperpolariability (β_{tot}) is 1.5 times higher than the value of urea. It has been found that the band gap energy is 3.96 eV. The anti-microbial studies shows that high activity (60%) against streptococcus viridians.

REFERENCES

[1] M. J. Berridge, "Inositol trisphosphate and calcium signalling mechanisms", Biochimica et Biophysica Acta (BBA)-Molecular Cell Research, vol. 1793, **(2009)**, pp. 933.

[2] M. T. Kozinova, I. A. Demina, V. B. Krylov, I. I. Baskin I and M. P. Rubtsova, "Functional Analysis of the C-terminal Domain of the Human Protein Rpp30 Involved in ribonucleoprotein assembly", Nucleic Acids Research, vol. 50, no. 8, **(2022)**, pp. 4574-4600.

[3] P. Vijaya and K. R. Sankaran, "A combined experimental and DFT study of novel unsymmetrical azine 2-(4-methoxybenzylidene)-1-(1-(4-isobutylphenyl)ethylidene) hydrazine", Spectrochimica Acta Part A: Molecular and Biomolecular Spectroscopy, vol. 138, **(2015)**, pp. 460-473.

[4] D. Ponikwicka-Tyszko, E. Chrusciel, and K. Kiec-Kononowicza, "Cinnamomum zeylanicum and Cinnamon acid as novel strategies to fight against Candida species", Fitoterapia, vol. 122, **(2017)**, pp. 1-8.

[5] S. Kumar and A. K. Verma, "Pharmacological properties of cuminaldehyde", A review. Asian Journal of Pharmaceutical and Clinical Research, vol. 6, no. 3, **(2013)**, pp. 12-17.

[6] C. H. Lee, Y. H. Liu, C. H. Lin, T. C. Lin, M. J. Lai, T. C. Chen, H. C. Huang, C. C. Hsu, C. W. Chang, Y. Y. Chang, H. Y. Lin and C. C. Lai, "Design and synthesis of novel 9-(2-phenylethynyl)guanine derivatives as inhibitors of human telomerase", Bioorganic & Medicinal Chemistry Letters, vol. 17, no. 22, **(2007)**, pp. 6167-6172.

[7] J. Li, C. Han, Y. Xue, H. Yan and B. Yu, "Design, synthesis, and evaluation of novel guanine derivatives as inhibitors of human DNA polymerase α", Bioorganic & Medicinal Chemistry Letters, vol. 24, no. 14, **(2014)**, pp. 3128-3132. DOI: 10.1016/j.bmcl.2014.05.032.

[8] L. O. Klotz, X. Hou, C. Jacob and N. Buchner, "Guanine-based distinctive drug design: Novel targets for future antiviral and anticancer chemotherapy", Chem. Med. Chem., vol. 9, no. 9, **(2014)**, pp. 2021-2030.

[9] G. B. Elion, "Acyclovir: Discovery, Mechanism of Action, and Selectivity", Journal of Medical Virology, vol. 1, **(1993)**, pp. 2-6.

[10] G. B. Elion, P. A. Furman, J. A. Fyfe, Paulo de Miranda, Lilia Beauchamp and H. J. Schaeffer, "Selectivity of action of an antiherpetic agent, 9-(2-hydroxyethoxymethyl)guanine", Proc. Natl. Acad. Sci. USA Medical Sciences, vol. 74, no. 12, **(1977)**, pp. 5716-5720.

[11] Christian Gibert, Julie Bestman-Smith, Guy Boivin, "Resistance of herpesviruses to antiviral drugs: clinical impacts and molecular mechanisms", Drug Resistance Updates, vol. 5, **(2002)**, pp. 88-114.

[12] Lynne Strasfeld, Sunwen Chou, "Antiviral Drug Resistance: Mechanisms and Clinical Implications Antiviral", Drug Resistance, vol. 24, **(2010)**, pp. 413-437.

[13] J. Antona, Wagstaff, Diana Faulds and L. Karen, "Aciclovir A Reappraisal of its Antiviral Activity", Pharmacokinetic Properties and Therapeutic Efficacy Drugs, vol. 47, no. 1, **(1994)**, pp. 153-205.

[14] N. Subramanian, N. Sundaraganesan, J. Jayabharathi, "An investigation on the molecular structure, vibrational spectra and first order hyperpolarizability of 2-chloro-4-nitrophenol by ab initio HF and density functional methods", Spectrochimica Acta Part A, vol. 76, no. 2, **(2010)**, pp. 259-69.

[15] M. H. Jamroz, "Quantum chemical calculations of electronic absorption spectra of some azomethine dyes: Comparative study of TD-DFT, CIS, and ZINDO/S methods", Spectrochimica Acta Part A, vol. 114, **(2013)**, pp. 220-30.

[16] N. Sundaraganesan, E. Kavitha, S. Sebastian, J. P. Cornard, M. Martel, "Computational and experimental investigation of vibrational spectra (FTIR and FT-Raman), NBO, MEP analysis and thermodynamic properties of 2-bromo-4-nitro chlorobenzene", Spectrochimica Acta Part A, vol. 74, no. 1, **(2009)**, pp. 788-797.

[17] M. Elango, R. Parthasarathi, G. K. Narayanan, A. M. Sabeelullah, U. Sarkar, N. S. Venkatasubramanian, V. Subramanian, P. K. Chattaraj, "Molecule-in-a-box: how does confinement affect the electronic structure, stability, and reactivity of the encapsulated species", Journal of Chemical Sciences, vol. 117, no. 4, **(2005)**, pp. 369-378.

[18] T. Bhaskar, M. Shanmugasundari, P. Vijaya, N. Banumathi, "Synthesis of 2-(2-amino-1,3 – dihydroxypropane-2-ylamino)benzoic acid", Research Journal of Chemistry and Environment, vol. 26, no. 12, **(2022)**, pp. 146-153.

[19] T. Bhaskar , D. Gana Saraswathy, N. Banumathi, P. Vijaya, "Synthesis, Characterization and DFT study of 2-amino-2'(diphenylamino)- Propane-1,3-diol", Research Journal of Chemistry and Environment, vol. 27, no. 6, **(2023)** , pp. 74-79.